JOURNAL OF EXPERIMENTAL AND THEORETICAL PHYSICS, 2024, Vol. 165, No. 6, pp. 838–843

ORDER, DISORDER, AND PHASE TRANSITION IN CONDENSED MEDIA

THE INFLUENCE OF IRRADIATION OF XE IONS WITH ENERGY 167 MEV ON SUPERCONDUCTING PROPERTIES OF 2G HTS WIRES

© 2024 P. N. Degtyarenko[a, b*], V. A. Skuratov[c**], A. L. Vasiliev[d,e], A. V. Ovcharov[d***], A. M. Petrszhik[b,f****], V. K. Semina[c], S. Y. Gavrilkin[g*****], M. S. Novikov[c******], A. Y. Malyavina[h*******], V. A. Amelichev[b], A.Y. Tsvetkov[g]

[a] *Joint Institute for high temperature of RAS 125412, Moscow, Russia*
[b] *S-innovations LLC 117246, Moscow, Russia*
[c] *Joint institute for nuclear research 141989, Dubna, Moscow region, Russia*
[d] *National research center "Kurchatov institute" 123182, Moscow, Russia*
[e] *National Research University MPTI141701, Dolgoprudny, Moscow region, Russia*
[f] *Kotel'nikov Institute of Radio Engineering and Electronics of RAS, 125009, Moscow, Russia*
[g] *Lebedev Physical Institute of Russian Academy of Science, 119991, Moscow, Russia*
[h] *National Research Nuclear University MEPhI, 115409, Moscow, Russia*

** e-mail: degtyarenkopn@gmail.com*
*** e-mail: skuratov@jinr.ru*
**** e-mail: ovcharov.91@gmail.com*
***** e-mail: a.petrzhik@s-innovations.ru*
****** e-mail: gavrs@sci.lebedev.ru*
*******e-mail: msnovikov@jinr.ru*
********e-mail: ayu.malyavina@gmail.com*

Received September 14, 2023
Revised January 25, 2024
Accepted January 26, 2024

Abstract. Systematic studies of 2G HTS wires irradiated by high-energy 167 MeV Xe ions and fluences up to $1 \cdot 10^{12}$ cm^{-2} have been carried out. The optimal fluence value (the number of particles passing through 1 cm^2 of the sample surface) for obtaining the maximum critical current at different temperatures and external magnetic fields has been determined. An increase in the external magnetic field leads to a shift of the critical current peak towards higher fluences in the whole temperature range. The results of microstructural investigations by transmission electron microscopy and X-ray diffraction methods are given. It is shown that because of irradiation ion tracks with a diameter of about 5-8 nm are formed, acting as effective pinning centers. X-ray diffraction analysis indicates a decrease in texture sharpness under the influence of irradiation.

Keywords: *high temperature superconductor, critical current, irradiation, fluence, critical temperature, microstructure of HTS, ion tracks, morphology of HTS*

DOI: 10.31857/S004445102406e099

1. INTRODUCTION

Second-generation high temperature superconductor wire (2G HTS) is a film of HTS with a thickness typically of a few micrometers [1]. The superconductor $ReBa_2Cu_3O_{7-\delta}$ (where Re is a rare earth element) is deposited on a flexible metal substrate coated with buffer layers. The formation of buffer layer texture, necessary for oriented growth of the HTS film, is achieved either through the use of a RABiTS (Rolling Assisted Biaxially Textured Substrate) textured substrate or through IBAD (Ion Beam Assisted Deposition) technology. The HTS layer is covered with protective and shunting layers on top. The vast majority of modern applications of HTS wire involve their operation in strong external

magnetic fields, which significantly reduce the superconducting capabilities of the tapes [2]. The deterioration of HTS superconducting properties in the presence of magnetic fields is caused by the drift of Abrikosov magnetic vortices, which requires the creation of artificial pinning centers to prevent such vortices [3]. For this purpose, defects that locally suppress superconductivity are deliberately introduced into the superconductor [4]. When the non-superconducting core of a vortex encounters such a defect, the vortex becomes pinned. Various approaches to creating artificial pinning centers are known, involving the use of different types of defects [5–8]. One of the most studied methods is the introduction of non-superconducting phase nano-inclusions with perovskite structure in the form of so-called nanocolumns $BaZrO_3$ [9] or $BaSnO_3$. This work examines the features and prospects of radiation pinning application with emphasis on flux optimization for various external conditions of temperature and magnetic field. The samples used were 4 mm wide sections of industrial 2G HTS wire manufactured by S-Innovations [11] with a silver protective layer. The irradiation technique is described in detail in works [12, 13], which also address the determination of optimal irradiation energy for tapes manufactured by Superpower.

2. SAMPLES AND EXPERIMENTAL METHODOLOGY

Square-shaped samples 3 mm × 3 mm were cut from industrial 2G HTS wire with a width of 4 mm. The tape manufactured by S-Innovations consisted of a flexible substrate (Hastelloy), buffer layers, a superconducting layer YBa2Cu3O7 with a thickness of about 2 μm and an upper protective Ag layer with a thickness of about 0.5 μm. The manufacturing technology is detailed in [1, 11].

The samples were irradiated with ions ^{132}Xe with energy of 167 MeV. The fluence value varied from $3 \cdot 10^{10}$ to $1 \cdot 10^{12}$ cm^{-2}. Irradiation with Xe ion flux of about $2 \cdot 10^{8}$ cm$^{-2} \cdot$ s^{-1} was carried out at room temperature using the IC-100 cyclotron at the Laboratory of Nuclear Reactions, JINR.

X-ray structural analysis was performed using a Rigaku SmartLab diffractometer with a rotating copper anode. All measurements were carried out in parallel beam geometry with Ge(220)×2 monochromator (wavelength $\lambda Cu_{K\alpha 1}$ = 1.541 Å).

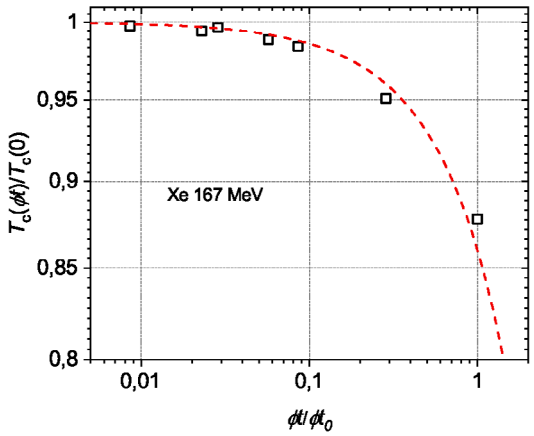

Fig. 1. Dependence of the normalized critical temperature of the superconducting transition of 2G HTS samples versus the normalized fluence value of Xe ions with energy of 167 MeV. Points – experimental data, dashed curve – dependence $T_c \approx T_{cO}(1 - k(\varphi t))$, $k \approx 0.14 \cdot 10^{12}$, where, T_{cO} – critical temperature of non-irradiated sample

Phase analysis and out-of-plane film orientation analysis were performed using 2Theta/Omega scanning. Omega scanning (so-called "rocking curves") was measured for (005) reflections of phase $YBa_2Cu_3O_7$ in the rolling direction (RD) and transverse direction (TD). Analysis of rocking curve widths allowed evaluation of the HTS film texture sharpness out of the substrate plane. Determination of the superconducting film texture sharpness in the substrate plane was performed using Phi- scanning for the (103) reflection of phase $YBa_2Cu_3O_7$ (2Theta = 32.5°, sample tilt angle Chi=45.3°). For each sample, preliminary spatial alignment was performed (maximizing reflection position for YBCO (005) reflection). The measurements and subsequent processing of results (determining FWHM parameter for rocking curves and Phi-scans) were carried out using standard software packages SmartLab Guidance and Integral Intensity Calculation.

Microstructural studies were carried out using a Tecnai Osiris transmission/scanning electron microscope at an accelerating voltage of 200 kV. Cross-sectional and planar sections for the studies were prepared using focused ion beam Ga^+ on focused ion beam scanning electron microscope Helios Nanolab 600.

3. RESULTS AND DISCUSSION

The dependence of the normalized value of the critical temperature of the superconducting transition, shown in Fig. 1, demonstrates a monotonic decrease T_c with increasing fluence. The dependence of the critical temperature on the irradiation dose is noted $T_c \approx T_{cO}(1 - k(\varphi t))$, $k \approx 0.14 \cdot 10^{12}$, where T_{cO} – critical temperature of non-irradiated sample. The decrease in T_c begins at fluence $8 \cdot 10^{10}$ cm^{-2} and at fluence $1 \cdot 10^{12}$ cm^{-2} decreases by 4 percent to 84.5 K (see table). Such behavior is associated with the formation of ion tracks, which cause deterioration in the sharpness of sample texture. At the same time, the created ion tracks are effective pinning centers for the vortex structure, which leads to an increase in the current-carrying capacity of the samples.

Fig. 2a shows the experimental dependencies of normalized (to non-irradiated sample under conditions of 77 K, 0T) critical current values on the normalized Xe ion fluence at temperatures of 77, 65, and 20 K in a field of 1 T. The nature of dependencies for the presented temperatures is similar, with curve maxima corresponding to the optimal fluence for the given field of about $2 \cdot 10^{11}$ cm^{-2}.

At $T = 20$ K (see Fig. 2 b) in a field of 1 T, the critical current peak is in the fluence region , and with increasing field noticeably shifts and at 8 T corresponds to the fluence region $3 \cdot 10^{11}$ cm^{-2}, and with increasing field noticeably shifts and at 8 T corresponds to the fluence $5 \cdot 10^{11}$ cm^{-2}. The observed behavior of the critical current is associated with an increase in the concentration of ion tracks acting as effective pinning centers. Thus, irradiation leads to the formation of a higher density of ion tracks with length of the order of HTS film depth (the Bragg range of such ions is several μm). With increasing fluence, the number of formed ion tracks increases, and the distance between them becomes comparable to 2λ (λ – penetration depth). It is at this distance that the maximum increase in collective pinning force occurs, i.e., the peak effect in critical current. According to work [15], for non-irradiated samples $YBa_2Cu_3O_7$ penetration depth at T = 0 K is 150 nm. According to our data for the sample irradiated with Xe ions with fluence $3 \cdot 10^{11}$ cm^{-2}, the penetration depth is 30 nm. The estimation was made from the relation for the second Fig. 4. critical field ($H_{c2} = \Phi_O/(\pi\lambda^2)$), which value was obtained from

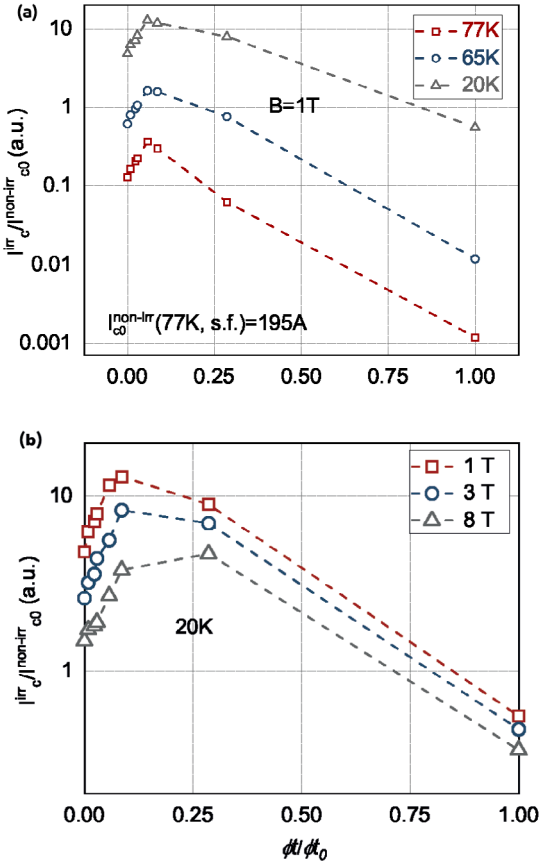

Fig. 2. Dependencies of the normalized critical current of 2G HTS wire samples on the normalized value of Xe ion fluence with energy of 167 MeV: a – in a field of 1 T and at temperatures of 77, 65 K and 20 K; b - in fields of 1, 3 and 8 T and temperature of 20 K

experimental data by plotting the superconducting transition temperature versus external magnetic field. The sample exhibits elastic inter-vortex interaction state, which contributes to maximum increase in current- carrying capacity. For clarity, the table shows maximum critical current values I_c , obtained for three characteristic external conditions: at $B = 0$, $T = 77$ K fluence $1 \cdot 10^{11}$ cm^{-2} gives $I_c = 274$ A, at $B = 2$T, $T = 50$ K, optimum shifts to fluence $2 \cdot 10^{11}$ cm^{-2} (735 A), and at $B = 8$ T, $T = 20$ K, – up to $5 \cdot 10^{11}$ cm^{-2} (critical current 921 A). The table shows that at high fluences, the critical current I_c at 77 K in self-field and critical temperature begin to decrease significantly due to superconductor structure degradation.

Figure 3 shows microstructure images of the sample irradiated with Xe ions with fluence cm $3 \cdot 10^{11}$ cm^{-2}, at different magnifications. The full-size cross-section image (Fig. 3*a*) clearly shows high film uniformity without any defects. In the magnified

Table 1: Parameters of non-irradiated and Xe ion-irradiated samples with different fluences. XRD RD and XRD TD are the rocking curve half-widths (005) YBCO along and across the tape, respectively. The XRD Phi column corresponds to the YBCO (103) reflection during Phi scanning. Maximum values are highlighted in bold with underline for various external condition

Fluence, cm^{-2}	I_c, A (4 mm, $B = 0$, 77 K),	I_c, A (4 mm, $B = 2$ T, 50 K)	I_c, A (4 mm, $B = 8$ T, 20 K)	T_c, K	XRD RD FWHM, deg.	XRD TD FWHM, deg.	XRD Phi FWHM, deg.
0	195	207	291	88	1.129	1.350	2.86
3×10^{10}	195	257	336	88	1.144	1.887	3.39
8×10^{10}	233	368	400	87.8	1.163	2.33	3.81
1×10^{11}	**274**	455	496	87.7	1.175	2.413	4.53
2×10^{11}	270	**735**	734	87.4	1.227	5.346	5.03
3×10^{11}	198.5	635	725	87	1.179	3.079	4.39
5×10^{11}	171	644	**921**	86.5	1.192	4.359	5.29
1×10^{12}	63	397	906	84.5	1.268	5.294	5.89

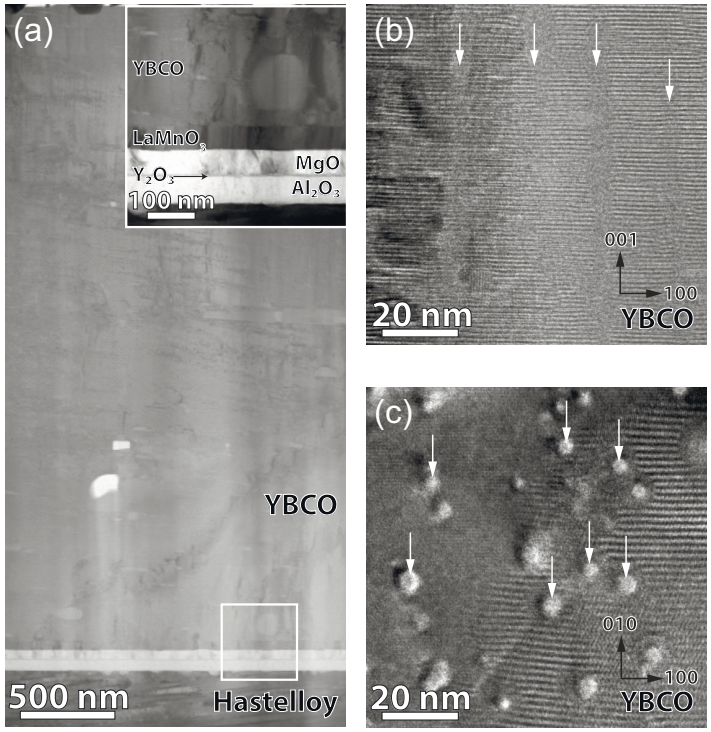

Fig. 3. Bright-field scanning transmission electron microscope (STEM) images of HTS wire full-size cross-section (a); inset shows magnified image of substrate/buffer layers/HTS interface. Transmission electron microscope (TEM) images of cross-sectional (b) and planar (c) sections of HTS layer. White arrows in the images indicate defects forming in the HTS matrix after Xe ion irradiation

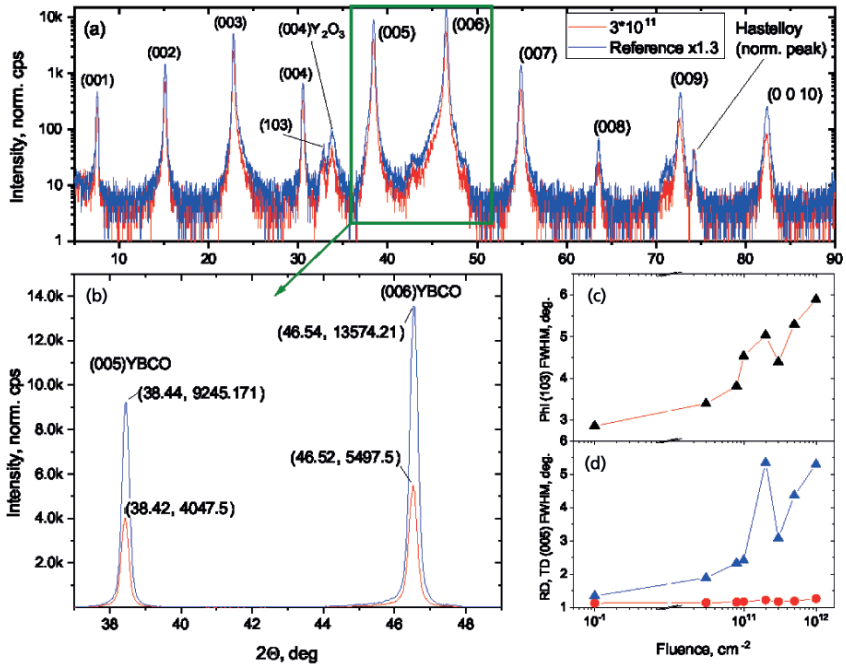

Fig. 4. a – X-ray diffraction patterns taken in symmetric Theta/2Theta mode for initial (non- irradiated) and Xe ion-irradiated samples with fluence of $3 \cdot 10^{11}$cm^{-2} . "Norm. peak" is the substrate reflection used for intensity normalization. b - Magnified area of figure a, which shows in detail the significant change in intensity of YBCO (005) and (006) reflections before and after irradiation. c - Average FWHM values of YBCO (103) reflection during Phi-scanning depending on fluence value. d - FWHM of rocking curve (005)YBCO in parallel (RD) and perpendicular (TD) directions to the tape depending on fluence value

TEM image of the cross-section of HTS film, ion tracks can be noticed, appearing as amorphous vertical nanocolumns with diameter of about 6 nm (Fig. 3b). For better track visualization, TEM images of the planar section of HTS layer were obtained, which clearly show rounded amorphous regions (Fig. 3c). It should be noted that there is a small variation in track diameters and their partial overlap.

Figure 4 shows diffraction patterns taken in symmetric mode on a Rigaku Smart Lab diffractometer. In Fig. 4*a* it is evident that the peak positions of the initial and irradiated samples (as an example, the diffraction pattern is shown for a sample irradiated with Xe ions with a fluence of $3 \cdot 10^{11}$ cm^{-2}) are practically indistinguishable, meaning that the crystal lattice parameter c does not change under irradiation. However, the peak widths increase significantly, indicating a decrease in texture sharpness, see the approximated area in Fig. 4*b*. Comparison of diffraction peak widths and their amplitudes is correct considering the same sample thickness and performed normalization by the substrate (Hastelloy) reflection amplitude. The deterioration of texture sharpness with increasing fluence is also confirmed by the Phi-scan (103) YBCO (see Fig. 4*c*). Notable is the different character of peak width increase in rocking curves (005)YBCO in parallel (RD) and perpendicular (TD) directions to the tape depending on the fluence value: in the non-irradiated sample, the rocking curves in two perpendicular directions (RD and TD) have approximately the same width, while in irradiated samples, there is a definite broadening in the TD direction. Such behavior confirms that an amorphous structure of regular tracks with a slight inclination relative to the crystallographic plane *ab* is realized in the sample.

4 CONCLUSION

Thus, systematic studies of electrophysical parameters and microstructure of samples before and after irradiation with Xe ions with previously determined [12] energy of 167 MeV and fluences up to $1 \cdot 10^{12}$ cm^{-2} have been conducted. The optimal fluence values at which peak of critical current values are observed for various external conditions have been established. It has been found that with increasing fluence, the critical current peak shifts towards stronger magnetic fields. Based on microstructural studies, it was revealed that ion tracks with a diameter of about 6 nm are formed as a result of irradiation. The formed tracks are effective

pinning centers, which is confirmed by the analysis of hysteresis magnetization curves of irradiated samples and the results of their morphology studies. A decrease in texture sharpness is observed with increasing fluence. The obtained results are planned to be used for calculating the necessary tape winding speeds directly through the ion beam, which will allow creating 2G HTS wires with increased current-carrying capacity due to the conducted radiation pinning.

FUNDING

The work was carried out with the support of the Ariadna MSTE collaboration under the applied materials science research program. X-ray phase analysis was conducted by

A.M.P. with financial support from the Russian Science Foundation (project No. 23-49-10006). Magnetic measurements were performed at the Shared Research Facility of the Lebedev Physical Institute RAS. Electron microscopy studies were carried out using the equipment of the Resource center of probe and electron microscopy (Kurchatov complex of NBICS-natural-like technologies, NRC "Kurchatov institute") and analysis of the obtained results were carried out with financial support from the Ministry of Science and Higher Education (State Assignment of JIHT RAS No. 075-01129-23-00).

REFERENCES

1. Markelov, A.; Valikov, A.; Chepikov, V.; Petrzhik, A.; Massalimov, B.; Degtyarenko, P.; Uzkih, R.; Soldatenko, A.; Molodyk, A.; Sim, K.; Hwang, S. 2G HTS Wire with Enhanced Engineering Current Density Attained through the Deposition of HTS Layer with Increased Thickness. Progress in Superconductivity and Cryogenics 2019, 21 (4), 29–33. https://doi.org/10.9714/PSAC.2019.21.4.029.
2. Malozemoff, A. P. Second-Generation High-Temperature Superconductor Wires for the Electric Power Grid. Annu. Rev. Mater. Res. 2012, 42 (1), 373–397. https://doi.org/10.1146/annurev-matsci-100511-100240.
3. Abrikosov, A. A. The Magnetic Properties of Superconducting Alloys. Journal of Physics and Chemistry of Solids 1957, 2 (3), 199–208. https://doi.org/10.1016/0022-3697(57)90083-5.
4. Blatter, G.; Feigel'man, M. V.; Geshkenbein, V. B.; Larkin, A. I.; Vinokur, V. M. Vortices in High-Temperature Superconductors. Rev. Mod. Phys. 1994, 66 (4), 1125–1388. https://doi.org/10.1103/RevModPhys.66.1125.
5. Selvamanickam, V.; Carota, G.; Funk, M.; Vo, N.; Haldar, P. High-Current Y-Ba-Cu-0 Coated Conductor Using Metal Organic Chemical-Vapor Deposition and Ion-Beam-Assisted Deposition. IEEE TRANSACTIONSON APPLIED SUPERCONDUCTIVITY 2001, 11 (I), 3379–3381. https://doi.org/10.1109/77.919787.
6. Catana, A.; Broom, R. F.; Bednorz, J. G.; Mannhart, J.; Schlom, D. G. Identification of Epitaxial Y2O3 Inclusions in Sputtered YBa2Cu3O7 Films: Impact on Film Growth. Appl. Phys. Lett. 1992, 60 (8), 1016–1018. https://doi.org/10.1063/1.106507.
7. MacManus-Driscoll, J. L.; Foltyn, S. R.; Jia, Q. X.; Wang, H.; Serquis, A.; Maiorov, B.; Civale, L.; Lin, Y.; Hawley, M. E.; Maley, M. P.; Peterson, D. E. Systematic Enhancement of In-Field Critical Current Density with Rare-Earth Ion Size Variance in Superconducting Rare-Earth Barium Cuprate Films. Applied Physics Letters 2004, 84 (26), 5329–5331. https://doi.org/10.1063/1.1766394.
8. Strickland, N. M.; Wimbush, S. C.; Kennedy, J. V.; Ridgway, M. C.; Talantsev, E. F.; Long, N. J. Effective Low-Temperature Flux Pinning by Au Ion Irradiation in HTS Coated Conductors. IEEE Trans. Appl. Supercond. 2015, 25 (3), 1–5. https://doi.org/10.1109/TASC.2014.2366079.
9. Erb, A.; Walker, E.; Flükiger, R. The Use of BaZrO3 Crucibles in Crystal Growth of the High-Tc Superconductors Progress in Crystal Growth as Well as in Sample Quality. Physica C: Superconductivity 1996, 258 (1–2), 9–20. https://doi.org/10.1016/0921-4534(95)00807-1.
10. Varanasi, C. V.; Barnes, P. N.; Burke, J.; Brunke, L.; Maartense, I.; Haugan, T. J.; Stinzianni, E. A.; Dunn, K. A.; Haldar, P. Flux Pinning Enhancement in YBa2Cu3O7−x Films with BaSnO3 Nanoparticles. Supercond. Sci. Technol. 2006, 19 (10), L37–L41. https://doi.org/10.1088/0953-2048/19/10/L01.
11. Molodyk, A.; Samoilenkov, S.; Markelov, A.; Degtyarenko, P.; Lee, S.; Petrykin, V.; Gaifullin, M.; Mankevich, A.; Vavilov, A.; Sorbom, B.; Cheng, J.; Garberg, S.; Kesler, L.; Hartwig, Z.; Gavrilkin, S.; Tsvetkov, A.; Okada, T.; Awaji, S.; Abraimov, D.; Francis, A.; Bradford, G.; Larbalestier, D.; Senatore, C.; Bonura, M.; Pantoja, A. E.; Wimbush, S. C.; Strickland, N. M.; Vasiliev, A. Development and Large Volume Production of Extremely High Current Density YBa2Cu3O7 Superconducting Wires for Fusion. Sci Rep 2021, 11 (1), 2084. https://doi.org/10.1038/s41598-021-81559-z.
12. Suvorova, E. I.; Degtyarenko, P. N.; Karateev, I. A.; Ovcharov, A. V.; Vasiliev, A. L.; Skuratov, V. A.; Buffat, P. A. Energy Dependent Structure of Xe Ion Tracks in YBCO and the Effect on the Superconductive Properties in Magnetic Fields. Journal of Applied Physics 2019, 126 (14), 145106. https://doi.org/10.1063/1.5120894.

13. Suvorova, E. I.; Degtyarenko, I. A.; Ovcharov, A. V.; Vasiliev, Influence of the Structure of Ion Tracks in YBCO on the Superconducting Properties of Composite Wires. Journal of Surface investigation 2022, 16 (1), 112-117. https://doi.org/10.1134/S1027451022010360.

14. Bean, C. P. Magnetization of Hard Superconductors. Phys. Rev. Lett. 1962, 8 (6), 250–253. https://doi.org/10.1103/PhysRevLett.8.250.

15. Larbalestier, D.; Gurevich, A.; Feldmann, D. M.; Polyanskii, A. High-Tc Superconducting Materials for Electric Power Applications. MATERIALS FOR SUSTAINABLE ENERGY 2010, 414. https://doi.org/10.1038/35104654.